Supplementary Information (SI) for Analyst.

Temporal SERS Quantification, Chemometric Monitoring of Amikacin Release in Blood Serum from Stimuli-Responsive Drug Carrier: Kinetics Modeling and In-Vitro Pharmacodynamic Evaluation

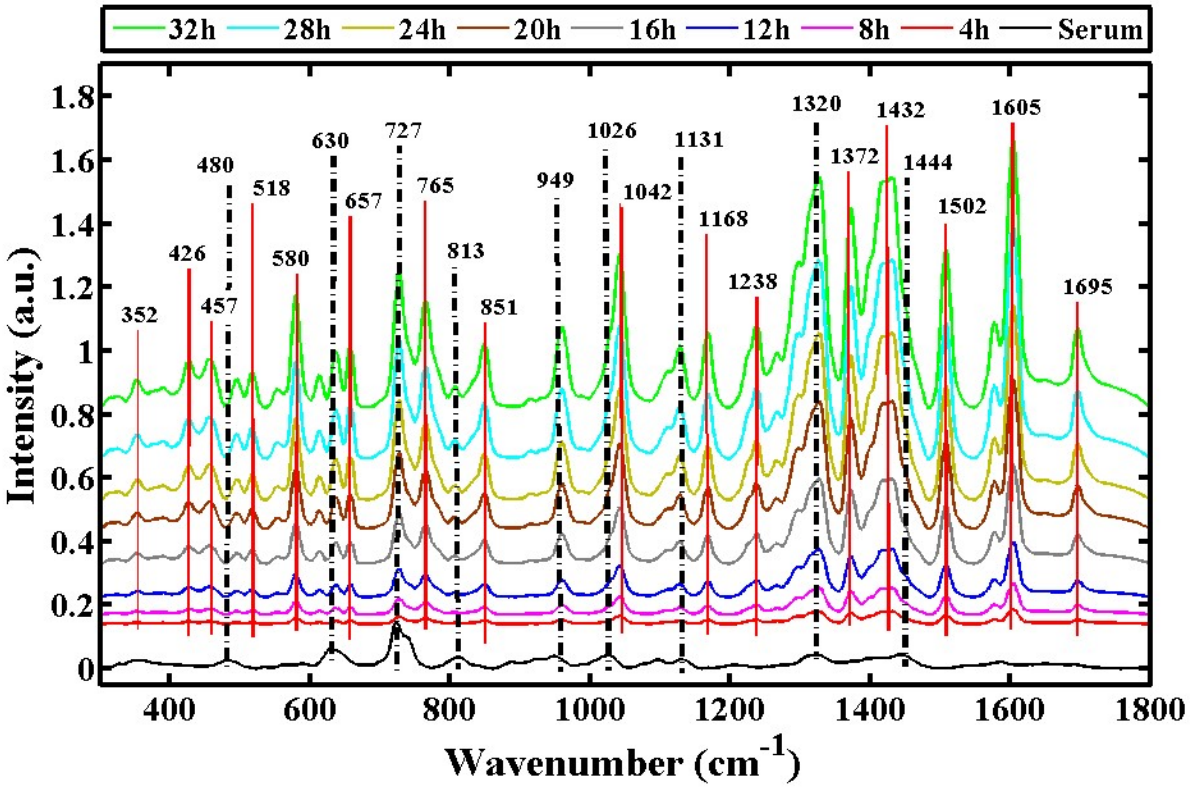

Fig. S1: The SERS mean spectra (detailed peak assignment) of AMK released from PVA/AgO Hydrogel in human blood Serum.

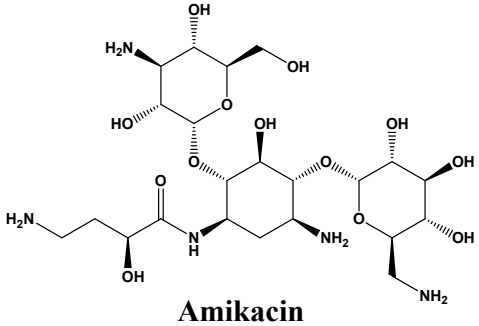

Fig. S2: The chemical structure of Amikacin (AMK).

Table S1: The tentative SERS peak assignments of the SERS bands from mean plot.

SERS Bands (cm^{-1})	SERS Assignment	Functional Group of AMK	References
352	Ring deformation	core of aminoglycoside	[1-3]
426	Skeletal bending vibration	C-C-O deformation in aminocyclitol ring	[3, 4]
457	Ring breathing vibration	aminoglycoside skeleton	[3, 5, 6]
480	C-O-C bending	Ether linkage between sugar units	[3, 7-10]
518	C-C skeletal stretch	Polyhydroxylated sugar ring framework	[11, 12]
580	C-N bending	Amino substituents on sugar rings	[13-16]
630	C-C-N bending	Amine group vibrations in aminocyclitol	[3, 17, 18]
657	C-O deformation	Secondary alcohol groups (-CHOH)	[16, 19]
727	Ring breathing	aminocyclitol (2-Deoxystreptamine) ring vibration	[3, 13, 16, 19]
765	C-O-C stretching	Glycosidic bond between sugar residues	[3, 13, 16, 20, 21]
813	C-O-C symmetric stretch	Bridge between sugar and amikacin side chain	[3, 13, 16, 20, 21]
851	C-H deformation	Anomeric carbon (sugar ring) vibrations	[11, 22]
949	C-O stretching	Alcohol and hydroxyl groups	[12, 23]
1026	C-N and C-O stretching	Amino sugar (glucosamine) backbone	[3, 5, 6]
1042	C-O-H bending	Primary and secondary	[3, 24]

		alcohol vibrations	
1131	C-N stretching	Amino group in glycosidic linkage	[25, 26]
1168	C-H bending	CH and CH_2 modes in sugar ring	[12, 25, 27]
1238	C–N–H deformation	Amino groups in deoxystreptamine ring	[3]
1320	CH_2 wagging and twisting	Aliphatic chain vibrations	[3, 27]
1372	CH_3 symmetric bending	Methyl groups (side chain vibrations)	[12, 26]
1432	CH_2 scissoring	C-H in aminosugar skeleton	[3, 11]
1444	CH_2 deformation	Aliphatic C-H stretch in side chain	[3, 23]
1502	N-H bending / C-N stretch	Amide linkage in acyl side chain	[13-16, 28]
1605	N-H bending and C=C stretch	Amide II and aromatic-type vibrations	[2, 12, 22]
1695	C=O stretching (Amide I band)	Acyl amide group in amikacin	[3, 6]

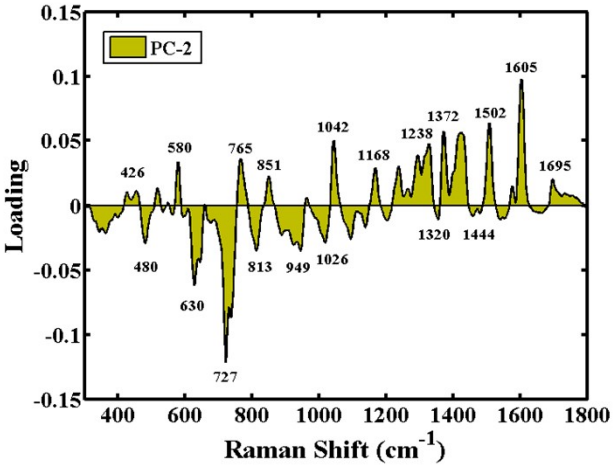

Fig. S3: The PC-2 plot of PCA analysis of SERS data.

Section 1. Optimization of Incubation Time for SERS Measurement

The **Fig.S4** shows how the incubation time can be optimized to measure the SERS spectra of AMK released in serum from PVA/AgO hydrogel. The Raman and SERS spectra (**Fig. S2(a)**) indicate that the intensity of the bands increases with the increase in the incubation time between 5 and 20 min, and then the signal sustained indicating that an adsorption equilibrium between the AMK molecules and the AgNPs surface is reached after 20 min and sustained after 25 and 30 min [5, 29-31]. This observation can also be illustrated by intensity difference box-plot (**Fig. S2(b)**) which shows the gradual growth of the median values of the intensities until 20 min, followed by the level, and the deceleration of the interquartile range indicates the steady acquisition of the signals [31, 32]. Also, the relative standard deviation (RSD %) (**Fig. S2(c)**) indicates an increase in spectral reproducibility as the incubation period increases, decreasing to values under 5% after 20 min. All these findings indicate that the best incubation time was 20 min, which is a compromise between amplification of the signals and accuracy of measurements, which ensures effective plasmonic coupling and homogenous adsorption of the molecules used in the quantitative chemical analysis of AMK release.

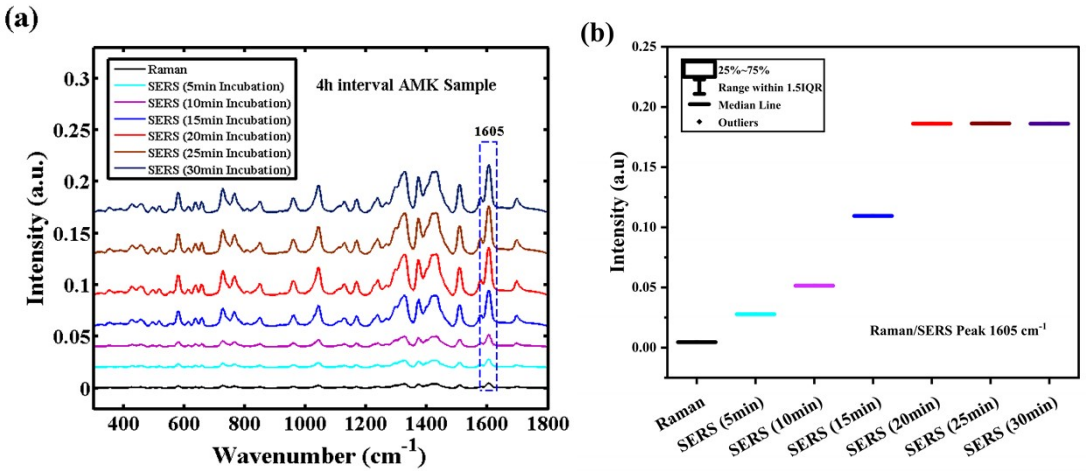

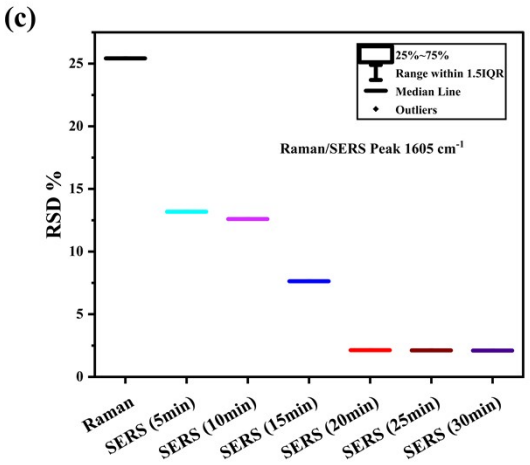

Fig. S4: Incubation time optimization of SERS measurement of AMK released in serum, **(a)** SERS spectra of AMK (4 h interval sample) at different incubation times (5-30 min) with normal Raman spectrum. **(b)** Boxplot analysis of intensity of SERS band at 1605 cm^{-1} that shows the median increase followed by stability thereafter, and **(c)** Relative standard deviation (RSD%) versus incubation time indicating that spectral reproducibility and stability have improved after 20 min.

Table S2. Comparative overview of recent chemometric SERS literature using PCA-PLSR to analyze quantitatively drugs or antibiotics.

Analyte / Application	**Chemometric Method**	**Sample / Matrix**	**Major Quantitative Findings**	**Reference**
Losartan Potassium (antihyperte	PCA + PLSR	Solid tablets	PLSR calibration $R^2 = 0.99$; RMSEC = 0.38 mg; RMSEP = 2.98 mg. Demonstrated accurate API quantification and batch uniformity	[33]

nsive)			via Raman-chemometric coupling.	
Sitagliptin (antidiabetic)	PCA + PLSR	Pharmaceutical solid form	R^2 = 0.99; RMSECV = 0.36 mg. Validated direct quantitative prediction in multicomponent excipient matrices.	[34]
Cefixime (broad-spectrum antibiotic)	PCA + PLSR	Commercial tablet formulations	Achieved R^2 = 0.99; RMSEC = 0.56 mg; RMSEP = 3.13 mg. Enabled discriminant and quantitative analysis of dosage forms.	[35]
Insulin degradation kinetics	PCA + PLSR	Liquid pharmaceutical formulation	PCA separated time-dependent degradation; PLSR R^2 = 0.98. Quantified storage-induced structural changes by SERS chemometrics.	[36]
Methyl Eugenol adulteration in pesticide formulation	PCA + PLSR	Liquid formulation	Quantitative adulterant detection with R^2 = 0.99; RMSEC = 1.9; RMSEP = 3.86. Demonstrated Raman-PLSR for trace contaminant control.	[37]
Methotrexate (anticancer drug)	PCA + PLSR (SERS-mapping)	Human serum	Quantitative SERS-PLSR ($R^2 \approx$ 0.98; LOD = 0.15 μM). Enabled simultaneous quantification of MTX and metabolites in clinical matrices.	[38]
Oxytetracycline	PCA + PLSR	PBS release medium	Linear SERS quantification validated with UV–Vis; $R^2 \approx 0.97$. Demonstrated chemometric tracking of hydrogel-mediated antibiotic	[31]

			release.	
Spectinomycin (SPM) and its Cu/Zn complexes	PCA + PLSR	PBS release medium	Multivariate model improved quantification accuracy over univariate analysis; R^2 > 0.98. Showed metal-complex influence on spectral variance.	[5]
Illicit drugs (amphetamine, cocaine, MDMA, heroin, methadone)	PCA (qualitative)	Street drug mixtures	PCA successfully classified five illicit drugs with >95% accuracy using SERS spectral fingerprints (1000–1800 cm^{-1}). Provided the foundational basis for PCA–PLSR in spectral chemometrics.	[39]
Amikacin (AMK) in PVA/AgO hydrogel (controlled release)	PCA + PLSR	Serum (in-vitro pharmacokinetics)	Real-time quantitative monitoring of AMK release; PLSR R^2_cal = 0.9765, R^2_val = 0.8731, RMSEC = 0.87, RMSEP = 0.88. Demonstrated diffusion-controlled release tracking in biological matrix.	**Current work**

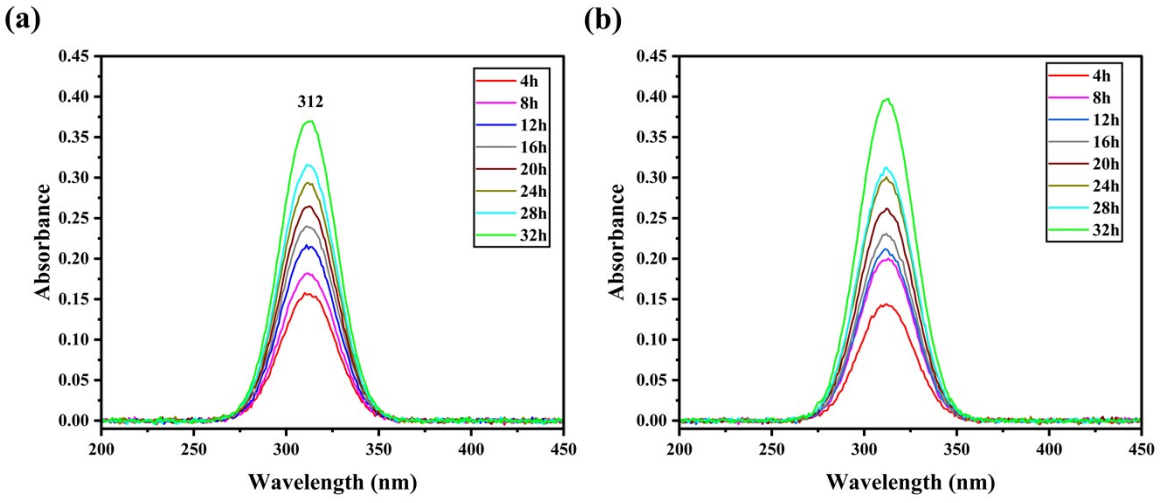

Fig. S5: UV vis absorption spectra of Amikacin (AMK) that were emitted in PVA/AgO hydrogel in **(a)** blood serum and **(b)** phosphate-buffered saline (PBS) at the various intervals (4 to 32 h). The corresponding blank media (serum or PBS), were used as the reference to record the spectra in the range of 200-600 nm to remove the background absorption. Both media have a typical AMK absorption peak of 312 nm in which intensity increases with time, which proves that the drug releases over time. The reference blanks did not give any spectral interference.

References

1. Ramirez, M.S. and M.E. Tolmasky, *Amikacin: uses, resistance, and prospects for inhibition.* Molecules, 2017. **22**(12): p. 2267.
2. Seely, S.M., et al., *Molecular basis of the pleiotropic effects by the antibiotic amikacin on the ribosome.* Nature communications, 2023. **14**(1): p. 4666.
3. Balan, C., L.-C. Pop, and M. Baia, *IR, Raman and SERS analysis of amikacin combined with DFT-based calculations.* Spectrochimica Acta Part A: Molecular and Biomolecular Spectroscopy, 2019. **214**: p. 79-85.
4. Nagarajan, T. and S. Jayakodi, *and Challenges.* Smart Nanosensors, 2025: p. 423.
5. Naman, A., et al., *SERS-Driven Chemometric Comparative Monitoring, Kinetics Study from Stimuli-Responsive Nanobiocomposite, DFT, Molecular Docking, and Biological Potential of Spectinomycin and Its Metal Complexes.* Plasmonics, 2025: p. 1-27.
6. Zhou, Y., Y. Ji, and Z. Cao, *Recent advances in optical detection of aminoglycosides.* Applied Sciences, 2020. **10**(18): p. 6579.
7. Miskowski, V., et al., *Copper coordination group in blue copper proteins. Evidence from resonance Raman spectra.* Biochemistry, 1975. **14**(6): p. 1244-1250.
8. Ramírez-Contreras, D., et al., *D, L-Citrullinato-bipyridine Copper Complex: Experimental and Theoretical Characterization.* Crystals, 2023. **13**(9): p. 1391.
9. Ali, A., et al., *Quantitative analysis of solid dosage forms of Atenolol by Raman spectroscopy.* Drug Development and Industrial Pharmacy, 2024. **50**(7): p. 619-627.
10. Shahbaz, M., et al., *Qualitative and Quantitative Analysis of Azithromycin as Solid Dosage by Raman Spectroscopy.* ACS omega, 2023. **8**(39): p. 36393-36400.
11. Wang, Q., et al., *A new perspective on antimicrobial therapeutic drug monitoring: Surface-enhanced Raman spectroscopy.* Talanta, 2025: p. 128017.

12. López-Díez, E.C., et al., *Monitoring the mode of action of antibiotics using Raman spectroscopy: investigating subinhibitory effects of amikacin on Pseudomonas a eruginosa.* Analytical chemistry, 2005. **77**(9): p. 2901-2906.
13. Fá, A.G., et al., *Detection of oxytetracycline in honey using SERS on silver nanoparticles.* TRAC Trends in Analytical Chemistry, 2019. **121**: p. 115673.
14. Meng, F., et al., *Ultrasensitive SERS aptasensor for the detection of oxytetracycline based on a gold-enhanced nano-assembly.* Talanta, 2017. **165**: p. 412-418.
15. Chen, S., et al., *Sensitive aptamer SERS and RRS assays for trace oxytetracycline based on the catalytic amplification of CuNCs.* Nanomaterials, 2021. **11**(10): p. 2501.
16. Zhang, R., et al., *Au-Ag alloy nanourchins as a highly efficient SERS tag synergistically with MOF@ Au for the ultrasensitive detection of oxytetracycline.* Journal of Colloid and Interface Science, 2025: p. 137840.
17. De Veij, M., et al., *Reference database of Raman spectra of pharmaceutical excipients.* Journal of Raman Spectroscopy: An International Journal for Original Work in all Aspects of Raman Spectroscopy, Including Higher Order Processes, and also Brillouin and Rayleigh Scattering, 2009. **40**(3): p. 297-307.
18. Chen, X., Y. Hu, and J. Gao, *Tautomers of 2-aminothiazole molecules in aqueous solutions explored by Raman, SERS and DFT methods.* Journal of Molecular Structure, 2013. **1049**: p. 362-367.
19. Lee, K.-M., et al., *Rapid detection and prediction of chlortetracycline and oxytetracycline in animal feed using surface-enhanced Raman spectroscopy (SERS).* Food Control, 2020. **114**: p. 107243.
20. Koleva, B.B., T.M. Kolev, and M. Spiteller, *Determination of cephalosporins in solid binary mixtures by polarized IR-and Raman spectroscopy.* Journal of pharmaceutical and biomedical analysis, 2008. **48**(1): p. 201-204.
21. Iliescu, T., M. Baia, and I. Pavel, *Raman and SERS investigations of potassium benzylpenicillin.* Journal of Raman Spectroscopy: An International Journal for Original Work in all Aspects of Raman Spectroscopy, Including Higher Order Processes, and also Brillouin and Rayleigh Scattering, 2006. **37**(1-3): p. 318-325.
22. McKeating, K.S., et al., *High throughput LSPR and SERS analysis of aminoglycoside antibiotics.* Analyst, 2016. **141**(17): p. 5120-5126.

23. Anjos, V.P., et al., *Identifying the Molecular Fingerprint of Beta-Lactams via Raman/SERS Spectroscopy Using Unconventional Nanoparticles for Antimicrobial Stewardship.* Antibiotics, 2024. **13**(12): p. 1157.
24. Tauber, A.L., S.S. Schweiker, and S.M. Levonis. *In vitro inhibitory evaluation of novel amine and amide compounds against the post-translational modifier enzyme, ARTD8*. in *The fourth Queensland Annual Chemistry Symposium (QACS 2019)*. 2019.
25. Qindeel, M., et al., *Nanomaterials for the diagnosis and treatment of urinary tract infections.* Nanomaterials, 2021. **11**(2): p. 546.
26. Wang, Z., *Surface-Enhanced Raman Scattering (SERS) Detection of Beta-Lactamase-mediated Antibiotic Resistance*. 2024, Queen's University (Canada).
27. Wasfi, R., et al., *Proteus mirabilis biofilm: development and therapeutic strategies.* Frontiers in cellular and infection microbiology, 2020. **10**: p. 414.
28. Hunt, B.C., et al., *Metabolic interplay between Proteus mirabilis and Enterococcus faecalis facilitates polymicrobial biofilm formation and invasive disease.* mBio, 2024. **15**(12): p. e02164-24.
29. Markovic, O.S., et al., *Nortriptyline hydrochloride solubility-pH profiles in a saline phosphate buffer: drug-phosphate complexes and multiple pHmax domains with a Gibbs phase rule "soft" constraints.* Molecular pharmaceutics, 2022. **19**(2): p. 710-719.
30. Mohan, C., *Buffers.* A guide for the preparation and use of buffers in biological systems, 2006: p. 20-1.
31. Mehmood, N., et al., *SERS Spectral Monitoring of Oxytetracycline In-Vitro Pharmacokinetics Quantification from Antibacterial Stimuli Responsive PVA/AgO Nanobiocomposite Hydrogel Along with Multivariate Data Analysis Techniques.* Plasmonics, 2025: p. 1-23.
32. Naman, A., et al., *Surface-enhanced Raman spectroscopy for characterization of supernatant samples of biofilm forming bacterial strains.* Spectrochimica Acta Part A: Molecular and Biomolecular Spectroscopy, 2024. **305**: p. 123414.
33. Shafaq, S., et al., *Quantitative analysis of solid dosage forms of Losartan potassium by Raman spectroscopy.* Spectrochimica Acta Part A: Molecular and Biomolecular Spectroscopy, 2022. **272**: p. 120996.

34. Bakkar, M.A., et al., *Raman spectroscopy for the qualitative and quantitative analysis of solid dosage forms of Sitagliptin.* Spectrochimica Acta Part A: Molecular and Biomolecular Spectroscopy, 2021. **245**: p. 118900.
35. Bajwa, J., et al., *Quantitative analysis of solid dosage forms of cefixime using Raman spectroscopy.* Spectrochimica Acta Part A: Molecular and Biomolecular Spectroscopy, 2020. **238**: p. 118446.
36. Meraj, L., et al., *Characterization of structural changes occurring in insulin at different time intervals at room temperature by surface-enhanced Raman spectroscopy.* Photodiagnosis and Photodynamic Therapy, 2023. **44**: p. 103796.
37. Anwar, M., et al., *Rapid identification and quantification of adulteration in methyl eugenol using raman spectroscopy coupled with multivariate data analysis.* ACS omega, 2024. **9**(7): p. 7545-7553.
38. Soufi, G., et al., *Discrimination and quantification of methotrexate in the presence of its metabolites in patient serum using SERS mapping, assisted by multivariate spectral data analysis.* Biosensors and Bioelectronics: X, 2023. **14**: p. 100382.
39. Tahira, M., et al., *Characterization of illicit drugs by surface-enhanced Raman spectroscopy (SERS) and principal component analysis (PCA).* Analytical Letters, 2024. **57**(16): p. 2713-2726.